

## A microwatt telemetry protocol for targeting deep implants

Kawasaki, Shinnosuke; Subramaniam, Indulakshmi ; Saccher, Marta; Dekker, Ronald

**DOI**

[10.1109/IUS52206.2021.9593603](https://doi.org/10.1109/IUS52206.2021.9593603)

**Publication date**

2021

**Document Version**

Final published version

**Published in**

2021 IEEE International Ultrasonics Symposium (IUS)

**Citation (APA)**

Kawasaki, S., Subramaniam, I., Saccher, M., & Dekker, R. (2021). A microwatt telemetry protocol for targeting deep implants. In *2021 IEEE International Ultrasonics Symposium (IUS): Proceedings* (pp. 1-4). Article 9593603 (IEEE International Ultrasonics Symposium, IUS). IEEE.  
<https://doi.org/10.1109/IUS52206.2021.9593603>

**Important note**

To cite this publication, please use the final published version (if applicable).  
Please check the document version above.

**Copyright**

Other than for strictly personal use, it is not permitted to download, forward or distribute the text or part of it, without the consent of the author(s) and/or copyright holder(s), unless the work is under an open content license such as Creative Commons.

**Takedown policy**

Please contact us and provide details if you believe this document breaches copyrights.  
We will remove access to the work immediately and investigate your claim.

# A microwatt telemetry protocol for targeting deep implants

Shinnosuke Kawasaki  
Microelectronics  
Delft University of Technology  
Delft, the Netherlands  
shinnosuke.kawasaki@philips.com

Ronald Dekker  
Microelectronics  
Delft University of Technology  
Delft, The Netherlands  
ronald.dekker@philips.com

Indulakshmi Subramaniam  
Microelectronics  
Delft University of Technology  
Delft, The Netherlands  
indulakshmi.subramaniam@philips.com

Marta Saccher  
Microelectronics  
Delft University of Technology  
Delft, The Netherlands  
marta.saccher@philips.com

**Abstract**—Implantable medical devices are becoming smaller and more deeply implanted in the human body for various applications (i.e., neurostimulation, drug delivery, bone fracture monitoring). Therefore, an efficient ultrasound power transfer link is needed to charge these devices. However, this is challenging because each ultrasound transducer has limited angular sensitivity. This work proposes a low-power telemetry protocol that can reliably feedback the power sent to the implant with backscattered ultrasound. The protocol works by sending two consecutive interrogation signals and connecting a circuit on the receiver that modulates only one of the two signals. The modulated signal can be decoded with an external ultrasound probe. In this work, the circuit was built, verified, and compared with simulation results. It was shown that the telemetry protocol could accurately localize the receiving ultrasound element at sub-mm precision at a 10 cm depth.

**Keywords**—pre-charged CMUT, backscattering, ultrasound power transfer, implantable medical device

## I. INTRODUCTION

Autoimmune diseases or neuropathic disorders are conventionally treated with pharmacological interventions. In recent years, implantable medical devices, such as neural stimulators, have been shown to be effective for the treatment of such diseases. Compared to pharmacological treatments that target the entire body, neural stimulation can be focused at the target location, enabling a selective therapy with fewer side effects. Several groups have worked on mm-size implantable devices that target deep innervations [1]–[3].

These mm-size deeply implanted medical devices use externally provided ultrasound power to operate. Ultrasound is safe to use in the body, and it has a high penetration depth and short wavelength, leading to a small focal point. However, establishing an efficient ultrasound power transfer link is still a challenge. The first approach to power a mm-size implant would be to rely on ultrasound imaging to obtain an accurate visualization of the implant position. However, the implant receiver for ultrasound has a limited angular sensitivity which requires good alignment and precise beam steering. In addition, the orientation of the receiver cannot be easily interpreted from the ultrasound image.

An alternative is to use time-reversal beamforming [4]. This is a simple and computationally efficient method that can accurately focus acoustic energy regardless of tissue scattering or tissue inhomogeneity. However, this method does not provide an absolute measure of the power sent to the implant,

and in most cases, it assumes that the implant can already operate without the initial ultrasound power.

As a result, a rapid feedback from the implant to the external transmitter is required to establish a power transfer link. This feedback could be in any form, either RF or ultrasound. However, considering the significant attenuation of RF within the body, several milliwatts of power will be required to transmit a signal that can still be detected from outside of the body. As a consequence, substantial time would be required for the energy to be harvested at the implant, creating an impractical inherent delay in the feedback loop.

In this work, we present a circuit that uses ultrasound backscattering to feedback information on the received power. This circuit operates in the microwatt range, and it feedbacks the voltage information on the storage capacitor of the implant within several milliseconds. Once the focus parameter is fixed, a tight ultrasound power transfer link will exist between the ultrasound transmitter and the receiver in which case this proposed circuit can be turned off for other functionalities.

## II. MICROWATT TELEMETRY PROTOCOL

Figure 1 shows how the microwatt telemetry protocol works. An interrogation signal is sent towards the ultrasound receiver from the external ultrasound probe at a pulse repetition frequency of 1kHz. The frequency of the ultrasound signal is 4 MHz, and bursts of 24 cycles are sent for a total duration of 6  $\mu$ s. The ultrasound receiver is loaded with a matching inductor, a modulation switch, and a modulation circuit. The detail on how this modulation circuit works is explained in the following section (II-A). Briefly, the backscattered signal from the ultrasound receiver is modulated with a time delay ( $\tau$ ) which is a function of the voltage on the storage capacitance ( $V_c$ ) for every other incoming burst. The demodulation process is done externally on MATLAB, and it is shown at the bottom of the same figure. The pulse width (PW) of the differential signal of two consecutive pulses encodes the information of the supply voltage as:

$$PW = T_{\text{burst}} - \tau(V_c) \quad (1)$$

where  $T_{\text{burst}}$  is the total duration of the ultrasound burst. By taking the differential signal at 1kHz pulse repetition frequency, common-mode interferences such as breathing, hand movements, or other low-frequency artifacts are removed, making a robust backscattering signal detection.

### A. Backscattering telemetry Circuit

The modulation circuit must accomplish two tasks. Firstly, the delay ( $\tau$ ) must be a function of the storage capacitance ( $V_c$ ), and secondly, the modulation must be applied to every other burst. Considering these two aspects, the circuit diagram shown on the right of figure 1 is the modulation circuit. In this circuit, the burst signal is first rectified, the envelope is detected with a Schmitt trigger (NXP Semiconductor, 74AUP2G17GW). Then, this envelope signal is connected to an RC low pass filter which delays the signal. The delay is defined by a 100 k $\Omega$  resistor and a variable capacitance diode (NXP Semiconductor, BB202, 10 pF to 30 pF) in series.  $V_c$  modulates the variable capacitance. Two variable capacitance diodes were used to increase the dynamic range, resulting in a capacitance change from 20 pF to 60 pF. After the envelope signal is delayed, the signal is connected to another Schmitt trigger to convert the signal into a well-defined pulse. This signal is then connected to the 1<sup>st</sup> input of an AND gate (NXP Semiconductor, 74AUP1G08GW). The output of the AND gate is connected to the gate of the modulation switch to modulate the backscattered signal with the modulated time delay. The modulation is applied to every other burst due to a toggle flipflop (NXP Semiconductor, 74AUP1G08GW) that is connected to the 2<sup>nd</sup> input of the AND gate. All the logic components are powered through the voltage on the storage

capacitor and have a total current consumption of around 0.5  $\mu$ A at 1 V operating voltage, thus only requiring microwatts of power consumption.

### B. Ultrasound backscattering setup

In figure 2a, the experimental setup that was used to validate the circuit is shown. A gel phantom (Rayher Hobby GmbH) with a 10 cm depth was positioned between the ultrasound transmitter (Philips, L7-4 linear probe) and the ultrasound receiver (RX). The ultrasound transmitter (TX) has 128 elements each of size 7 mm  $\times$  0.28 mm with a spacing of 25  $\mu$ m between each element. This results in a TX width of 4 cm. The RX consists of 6 Capacitive Micromachined Ultrasonic Transducer (CMUT) elements in parallel, each consisting of 56 cells. The size of the RX is 0.84 mm  $\times$  7.4 mm. TX and RX were aligned in the x and y-axis direction using a linear micromanipulator. The alignment was tuned by maximizing the output voltage seen at RX when the TX focused at (y, z) = (0 mm, 100 mm). The z-direction was adjusted by measuring the distance with a caliper. Figure 2b shows the cross section along the y-z plane at x = 0 when the ultrasound was focused at (y, z) = (0 mm, 100 mm). The red line corresponds to the width of RX. The simulated focal width and length was 0.88 mm and 17 mm respectively. Since the width of RX is nearly

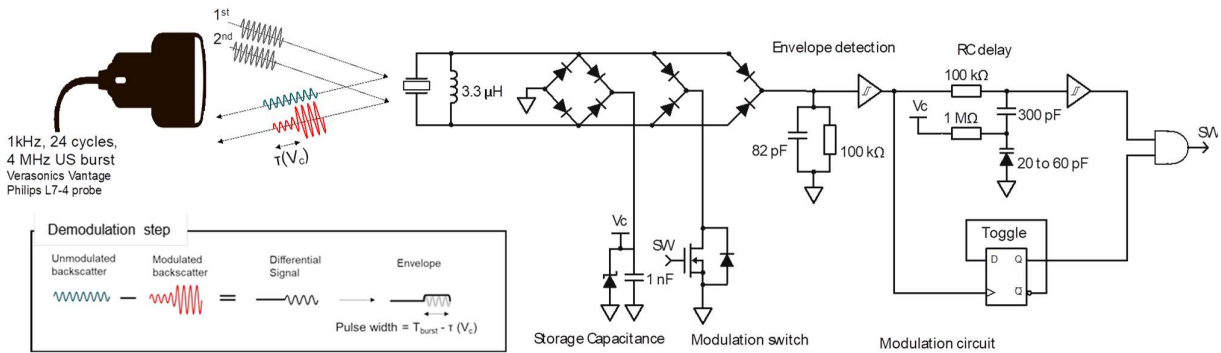


Figure 1 Ultrasound backscattering telemetry protocol. The voltage on the storage capacitance is encoded in the pulse width of the backscattered signal.

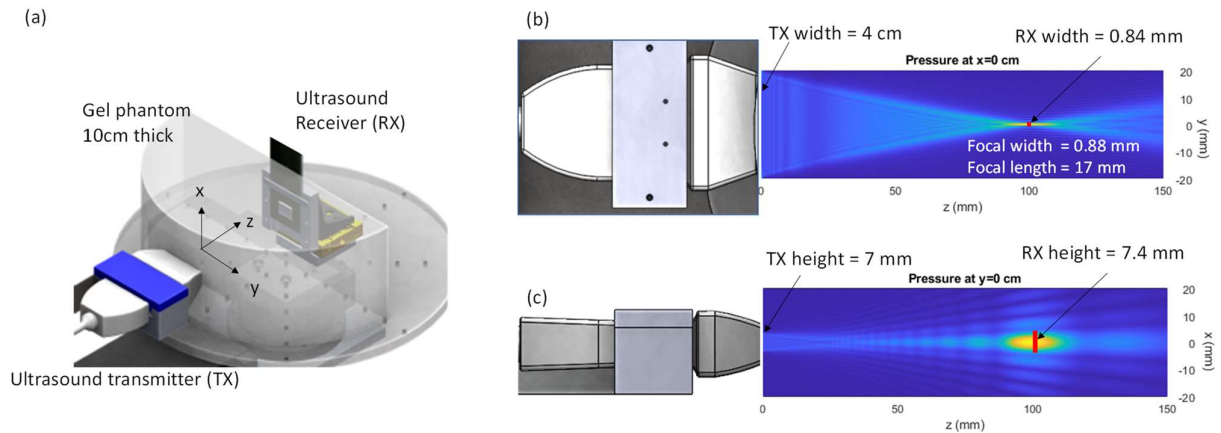


Figure 2 (a) Experiment setup with the Philips L7-4 probe sending ultrasound towards the CMUT through a 10 cm thick gel phantom. The xyz coordinate is defined as shown in the figure and the origin is defined at the center of the ultrasound transmitter. The simulated ultrasound profile is shown, (b) along the y-z plane at x = 0 and (c) along the x-z plane at y = 0. The receiving element is represented by a red line.

equal to the focal width, it shows how critical the beamforming parameters are to focus the power to RX. Figure 2c is the x-z plane at  $y = 0$  for the same focusing condition. The focus cannot be steered in this plane, and thus, the experimental setup is limited to a telemetry protocol within the y-z plane. This experimental setup and the microwatt telemetry protocol are used to measure how much power is sent to RX. The experimental results are also compared to simulations.

### III. RESULTS AND DISCUSSION

#### A. Using backscatter telemetry to read received power

Figure 3a is an example of the backscattered signal seen at TX when TX and RX are perfectly aligned. The modulated signal and the unmodulated signal are both shown in this figure. The waves are distorted due to reflections and scattering in the phantom, and it is not easy to decipher the modulation at this state. Thus, the differential signal and the envelope are taken to determine PW. In figure 3b, the relation between the pulse width and the voltage on the storage capacitor is shown for increasing voltage applied at TX. The voltage on the storage capacitance is proportional to the PW, which satisfied eq. 1 hence validating the functioning of this circuit.

The RX is then located by steering the beam from -2 mm to 2 mm along the y-axis and 80 mm to 150 mm in the z-axis in 55 steps in both axes. This corresponds to a spatial resolution of 0.07 mm and 1.27 mm along the y and z axes respectively. The measurement result is plotted in the form of a heatmap in figure 4a. Each 2D coordinate in the plot shows how long PW was when the beam was focused on each coordinate. From this heatmap the RX can be located to be  $(y, z) = (0 \text{ mm}, 100 \text{ mm})$  which is exactly what we expect (see the experimental setup in section II-B).

#### B. Simulating received ultrasound power

In addition, a simulation of the received ultrasound power was done in three steps. First, the acoustic pressure at the surface of the receiver was simulated assuming a lossless medium and continuous wave mode using Fast Object-oriented C++ Ultrasound Simulation (FOCUS)[5], [6]. Second, the acoustic pressure was averaged over the surface of the receiver,

including the phase information. Finally, the averaged acoustic pressure is converted to the total received power at the receiver by taking the square of the magnitude. These steps were repeated for different steering conditions and were normalized and plotted as a heatmap in figure 4b.

The results show that the main lobe at the center of figure 4 is similar, although it is noisier for the measurement result. The solid blue area in figure 4a shows that no backscatter modulated information was available for these regions. This is due to the limited dynamic range of the backscattering circuit. This can also be seen in figures 4c and 4d, which is the normalized received ultrasound power evaluated at  $z = 100 \text{ mm}$  and  $y = 0 \text{ mm}$ , respectively. The measurement result follows the simulation profile nicely as long as the received power is above 0.4. If the normalized received power is lower than this, the measurement circuit does not have enough dynamic range to follow the simulated results. It is also noticeable that the measurement profile is wider than the simulation results in both cross-sections. This could be due to rotational misalignments or other offsets.

In addition, the spatial peak temporal average intensity ( $I_{SPTA}$ ) used in this work was  $30 \text{ mW/cm}^2$ , which is below the FDA limit of  $720 \text{ mW/cm}^2$  for ultrasound imaging.

The backscatter telemetry protocol proposed in this work is simple and it is expected to work in numerous other settings. For example, if the implant needs to be localized in 3D this is possible if a 2D probe is used. Furthermore, the receiving transducer can be replaced with any other transducer or any other operating frequencies can be used.

Moreover, this system allows the transmission of other low data-rate information (i.e. temperature data, simple commands, identification code.) with this telemetry protocol, since the data rate of this system is half of the pulse repetition frequency, in this work 500 Hz.

### IV. CONCLUSION

In this work we have shown that the proposed microwatt telemetry protocol is able to communicate information of the amount of voltage on the storage capacitor to the ultrasound probe. The resolution of the power transfer was high enough to accurately send ultrasound energy to a sub-mm wide RX

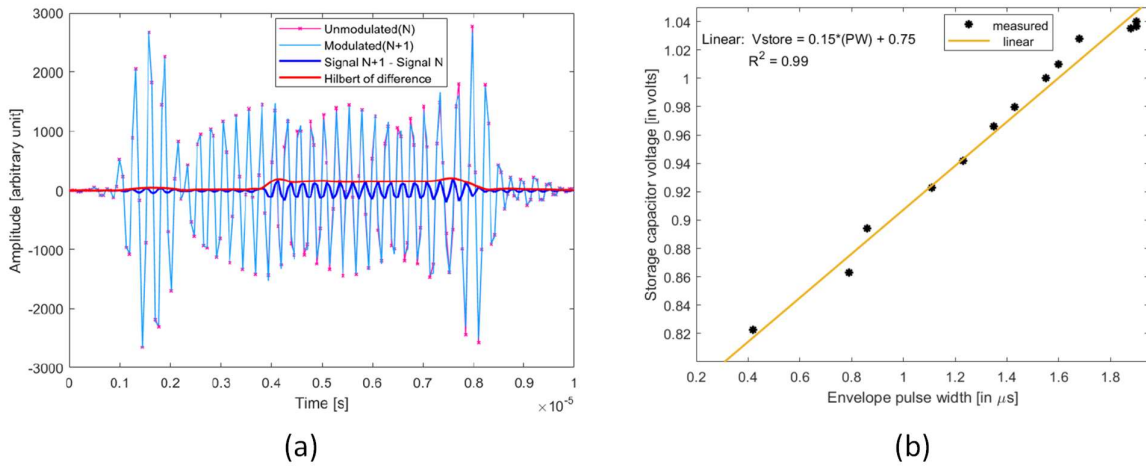


Figure 3 (a) Demodulation process of the voltage on the storage capacitance. (b) Linear relation between the pulse width and the storage capacitor voltage

element at a 10 cm depth. We will focus on testing this telemetry protocol in inhomogeneous mediums with vibrating motions to mimic a real-life use case for future work. We will extend this concept in order to differentiate between multiple implants that could be present in the body

#### ACKNOWLEDGMENT

The authors would like to thank the researchers working at Philips research. This project is funded by the ULIMPPIA and Moore4Medical projects. ULIMPPIA is labelled as a Penta Project Endorsed by Eureka under Penta cluster number E!9911 References. Moore4Medical receives funding from the ECSEL JU, under grant agreement H2020-ECSEL-2019-IA-876190.

#### REFERENCES

- [1] D. Seo *et al.*, “Wireless Recording in the Peripheral Nervous System with Ultrasonic Neural Dust NeuroResource Wireless Recording in the Peripheral Nervous System with Ultrasonic Neural Dust,” *Neuron*, vol. 91, no. 3, pp. 529–539, 2016, doi: 10.1016/j.neuron.2016.06.034.
- [2] B. D. Link, J. Charthad, S. Member, M. J. Weber, and S. Member, “A mm-Sized Implantable Medical Device (IMD) With Ultrasonic Power Transfer and a Hybrid,” *IEEE J. Solid-State Circuits*, vol. 50, no. 8, pp. 1741–1753, 2015, doi: 10.1109/JSSC.2015.2427336.
- [3] C. Shi *et al.*, “Wireless Sensing Mote for Real-Time Physiological Temperature Monitoring,” vol. 14, no. 3, pp. 412–424, 2020.
- [4] B. C. Benedict, M. M. Ghanbari, S. F. Alamouti, N. T. Ersumo, and R. Muller, “Time reversal beamforming for powering ultrasonic implants,” 2021.
- [5] R. J. McGough, “Rapid calculations of time-harmonic nearfield pressures produced by rectangular pistons,” *J. Acoust. Soc. Am.*, vol. 115, no. 5 Pt 1, pp. 1934–41, 2004, doi: 10.1121/1.1694991.
- [6] D. Chen, J. F. Kelly, and R. J. McGough, “A fast near-field method for calculations of time-harmonic and transient pressures produced by triangular pistons,” *J. Acoust. Soc. Am.*, vol. 120, pp. 2450–2459, 2006, doi: 10.1121/1.2356839.

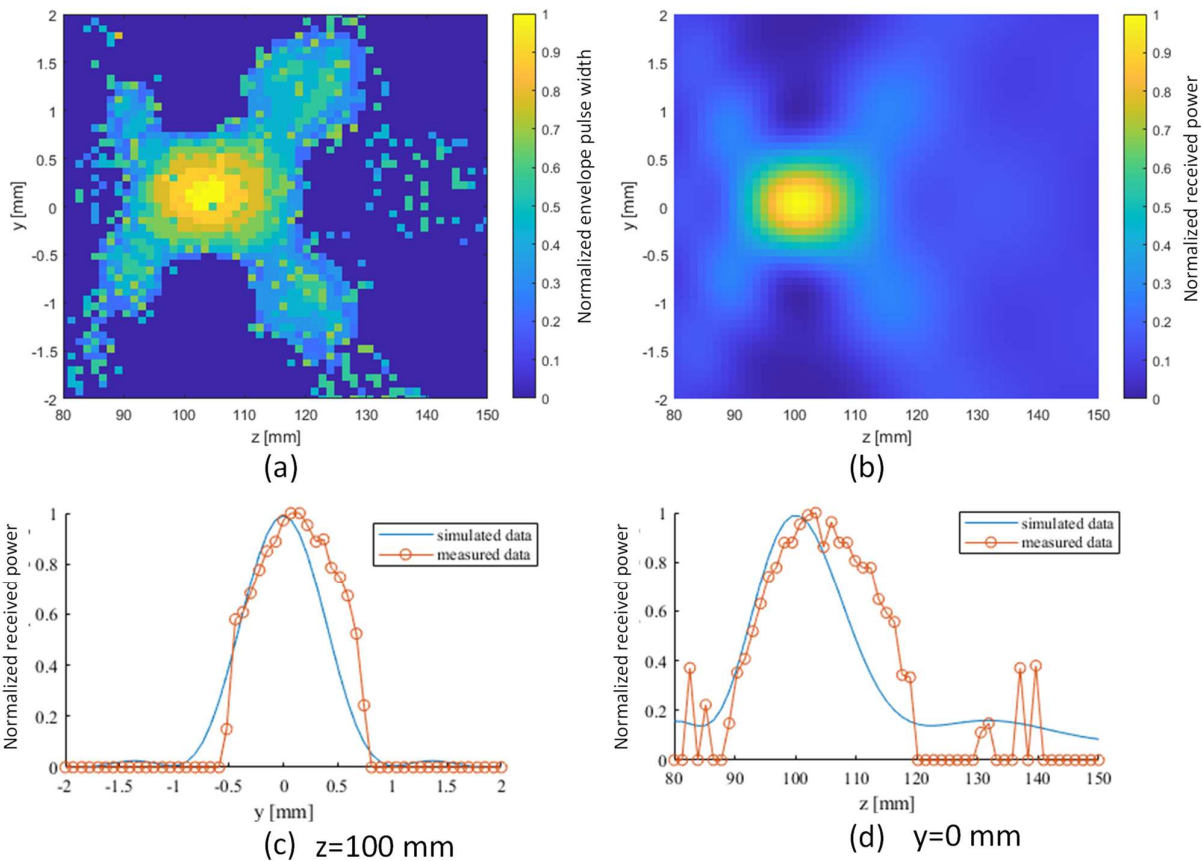


Figure 4 (a) Measured pulse width when the beam was steered in the y-z plane. (b) Simulated normalized received power simulated in the y-z plane. The normalized received power is compared along (c)  $z=100$  mm and (d)  $y=0$  mm.